

# ENVELOPE ESTIMATION BY TANGENTIALLY CONSTRAINED SPLINE

*Tsubasa Kusano, Kohei Yatabe and Yasuhiro Oikawa*

Department of Intermedia Art and Science, Waseda University, Tokyo, Japan

## ABSTRACT

Estimating envelope of a signal has various applications including empirical mode decomposition (EMD) in which the cubic  $C^2$ -spline based envelope estimation is generally used. While such functional approach can easily control smoothness of an estimated envelope, the so-called undershoot problem often occurs that violates the basic requirement of envelope. In this paper, a tangentially constrained spline with tangential points optimization is proposed for avoiding the undershoot problem while maintaining smoothness. It is defined as a quartic  $C^2$ -spline function constrained with first derivatives at tangential points that effectively avoids undershoot. The tangential points optimization method is proposed in combination with this spline to attain optimal smoothness of the estimated envelope.

**Index Terms**— Empirical mode decomposition (EMD), spline interpolation, quartic  $C^2$ -spline, constrained optimization, adjoint-state method.

## 1. INTRODUCTION

An envelope of a signal is a smooth wrapping curve containing much information about the signal, and therefore it is widely considered in signal processing [1]. One of the applications that envelope estimation plays a crucial role is empirical mode decomposition (EMD) [2]. It is a data-driven technique for non-stationary signal analysis [3–6] and has been applied in various fields [7–11].

The accuracy of EMD is determined by the accuracy of envelope estimation because subtraction of the mean of upper and lower envelopes is the central step in the process of EMD (see Sec. 2.1). The popular method for estimating envelopes in EMD and its variants [12–15] is based on the cubic  $C^2$ -spline interpolation [2–15]. Although this approach can obtain smooth envelopes, it suffers from the so-called undershoot problem which violates the basic requirement of envelopes and leads to erroneous results.

Many approaches have been proposed to replace the cubic  $C^2$ -spline interpolation so that the estimation accuracy of envelopes improves, such as B-spline [16], piecewise quadratic functions [17], segment power functions [18] and other spline functions [19–21]. However, these methods are often heuristic and lack discussion on optimality. On the other hand, approaches based on constrained optimization can incorporate desired properties through the constraint so that an optimal envelope is obtained [22–24]. Nevertheless, their models are usually too flexible for practical use because they involve an excessive number of parameters in contrast to the above functional approaches. An approach between the two should be a preferable choice, i.e., one that constrains an interpolation function but leads to a small number of parameters.

In this paper, an envelope estimation method using a quartic  $C^2$ -spline function constrained with first derivatives, named tangentially constrained spline, is proposed together with a gradient-based tangential points optimization method. The proposed method estimates an optimal envelope in terms of its smoothness while the undershoot problem is circumvented owing to the constraint.

## 2. PRELIMINARIES

### 2.1. Empirical mode decomposition (EMD)

EMD aims to decompose a multicomponent signal  $u(t)$  into intrinsic mode functions (IMFs)  $\{m_k(t)\}_{k=1}^M$ , which are locally zero-mean oscillatory components, and residual  $r(t)$  which represents trend. The algorithm of EMD proposed in [2] is summarized as follows:

Step 1. Initialize  $r(t) = u(t)$ , and  $k = 1$ .

Step 2. Extract the  $k$ th IMF  $m_k(t)$ :

(a) Initialize  $m_k(t) = r(t)$ .

(b) Find all local extrema of  $m_k(t)$ .

(c) Calculate upper envelope  $e_{\max}(t)$  (resp. lower envelope  $e_{\min}(t)$ ) by interpolating all maxima (resp. minima) using the cubic  $C^2$ -spline.

(d) Update  $m_k(t) = m_k(t) - (e_{\max}(t) + e_{\min}(t)) / 2$ .

(e) Repeat Steps (b)–(d) until it converges to an IMF.

Step 3. Update  $r(t) = r(t) - m_k(t)$ .

Step 4. Repeat Steps 2 and 3 with  $k = k + 1$  until the stopping criterion is satisfied.

The main process of EMD is subtraction of the mean value of upper and lower envelopes. Therefore, the accuracy of EMD is decided by the accuracy of envelope estimation.

### 2.2. Spline functions and cubic $C^2$ -spline interpolation

A spline is a continuous function defined by piecewise polynomials that has been widely used in signal processing owing to its flexibility and optimality [25]. Let an interval  $[x_0, x_n]$  be divided into  $n$  subintervals by a grid  $\mathbf{x} = [x_0, x_1, \dots, x_n]^T \in \mathbb{R}^{n+1}$  such that  $x_0 < x_1 < \dots < x_n$ , and let  $\rho, d \in \mathbb{Z}$  such that  $0 \leq \rho < d$ , where  $A^T$  denotes transpose of  $A$ . The set of  $\rho$  times continuously differentiable spline functions of degree  $d$  on grid  $\mathbf{x}$  is defined as

$$S_d^\rho(\mathbf{x}) = \{f \in C^\rho([x_0, x_n]) \mid f = f_k \in \mathbb{P}_d \text{ on } [x_k, x_{k+1}] \forall k\}, \quad (1)$$

where  $C^\rho(\Omega)$  is the set of  $\rho$  times continuously differentiable functions on  $\Omega$ , and  $\mathbb{P}_d$  is the set of all polynomials whose degree is at most  $d$ .

One of the reasons for spline's popularity comes from its optimality in terms of smoothness. Let us consider spline interpolation which is a problem of finding a spline function passing through all given points  $(x_k, y_k)$ . The most standard spline for this task is cubic  $C^2$ -spline,  $S_3^2(\mathbf{x})$ , because its interpolant is optimally smooth and characterized by a solution to the following optimization problem:

$$\begin{aligned} & \underset{s \in S_3^2(\mathbf{x})}{\text{minimize}} && \frac{1}{2} \int_{x_0}^{x_n} |s''(t)|^2 dt \\ & \text{subject to} && s(x_k) = y_k \text{ for all } k, \end{aligned} \quad (2)$$

where  $s''(t)$  denotes second derivative of  $s(t)$ . That is, a spline interpolant in  $S_3^2(\mathbf{x})$  automatically becomes the smoothest function among all cubic  $C^2$ -spline functions passing through the data points.

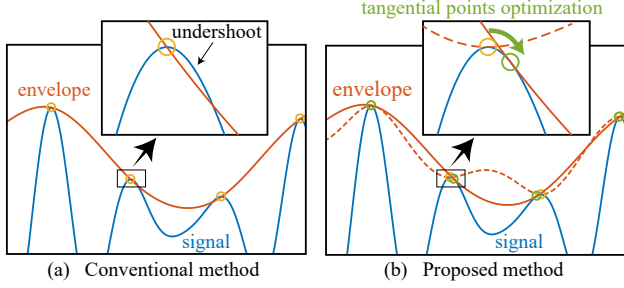


**Fig. 1.** Schematic of estimated envelopes obtained by (a) the conventional cubic  $C^2$ -spline interpolation, and (b) the proposed method.

### 2.3. Related research on envelope estimation

Since a spline function can handle smoothness easily as in the previous subsection, it has been widely adopted to the envelope estimation problems [2–15]. However, directly interpolating extrema as in the EMD algorithm in Sec. 2.1 often causes the so-called undershoot problem which is illustrated in Fig. 1 (a). The conventional envelope estimation by cubic  $C^2$ -spline interpolation in Fig. 1 (a) resulted in an envelope whose magnitude is below the signal at certain points. This is a violation of the definition of envelope which “wraps” the signal, i.e., an envelope must not cross the signal. Such undershoot is a great source of artifacts contaminating the results of EMD [26], and thus it should be avoided.

For estimating an envelope without undershoot, approaches based on constrained optimization have been proposed [23, 24]. Since these methods consider signal values at every sample point as optimization variables, various kinds of constraints promoting desired properties of envelope can be incorporated. Although such methods are quite flexible, they might be too time-consuming because the number of parameters usually becomes very large.

On the other hand, many methods based on spline functions have been proposed to avoid undershoot with less number of parameters [17–21]. One direction of this research is to modify the class of functions so that undershoot is circumvented [17–19]. However, such modification of the set of functions is somewhat heuristic, and it may not be easy to consider its optimality. Another notable direction of the research is based on first derivatives [20, 21]. These methods modify interpolation points so that first derivatives of an envelope at tangential points become close to those of the signal. This point of view is reasonable because the definition of an envelope in geometry usually contains such a tangential condition. However, they consider the tangential condition only approximately. In addition, they did not consider optimality on smoothness.

## 3. PROPOSED METHOD

In this section, we propose a tangentially constrained spline for envelope estimation (Sec. 3.1) that can be made optimally smooth by the proposed tangential points optimization (Sec. 3.2). Schematic explanation of the proposed method is shown in Fig. 1 (b), where the dotted red line represents the tangentially constrained spline which is tangent to signal at interpolation points. By optimizing the tangential points, it becomes optimally smooth as the thick red line in Fig. 1 (b) because the points are optimized based on its smoothness. In contrast to the previous research introduced in the previous subsection, the proposed method estimates an envelope which is strictly tangent at interpolation points and is optimally smooth.

### 3.1. Tangentially constrained spline for envelope estimation

One of the reasons that an estimated envelope has non-desirable features such as undershoot is neglect of the property of the envelope, that is, an envelope must be tangent to the signal at interpolation points. Since extrema are points where first derivative of the signal changes its sign, an interpolant of the maxima tangent to the signal at those points locally becomes an upperbound of the signal. Therefore, an envelope should be tangent at certain points around extrema of the signal.

Based on this observation, we propose *tangentially constrained spline*  $s_{TC}$  which is a quartic  $C^2$ -spline function constrained with first derivatives and characterized as an optimal solution of the following optimization problem:

$$\begin{aligned} & \text{minimize} && \frac{1}{2} \int_{\tau_0}^{\tau_n} |s''_{TC}(t)|^2 dt \\ & \text{subject to} && s_{TC}(\tau_k) = u(\tau_k) \\ & && s'_{TC}(\tau_k) = u'(\tau_k) \text{ for all } k, \end{aligned} \quad (3)$$

where  $\boldsymbol{\tau} = [\tau_0, \tau_1, \dots, \tau_n]^T \in \mathbb{R}^{n+1}$  denotes tangential points of  $u(t)$  such that  $\tau_0 < \tau_1 < \dots < \tau_n$ . In order to consider first derivative in addition to Eq. (2), the degree of the piecewise polynomials is increased from cubic,  $S_3^2(\boldsymbol{\tau})$ , to quartic,  $S_4^2(\boldsymbol{\tau})$ . By constraining the first derivative at the tangential points, the proposed spline is tangent to the signal at those points. The benefit of doing this will be demonstrated by an example in the next experimental section.

This problem can be discretized without any approximation thanks to the properties of spline. Let the optimization variables be written in the standard form as in [27]:

$$\mathbf{s} = [\mathbf{z}^T, \mathbf{p}^T, \mathbf{P}^T]^T \in \mathbb{R}^{3n+3}, \quad (4)$$

where  $\mathbf{z} = [z_0, \dots, z_n]^T \in \mathbb{R}^{n+1}$ ,  $\mathbf{p} = [p_0, \dots, p_n]^T \in \mathbb{R}^{n+1}$ ,  $\mathbf{P} = [P_0, \dots, P_n]^T \in \mathbb{R}^{n+1}$ ,  $z_k = s_{TC}(\tau_k)$ ,  $p_k = s'_{TC}(\tau_k)$ , and  $P_k = s''_{TC}(\tau_k)$ . Then, the integration in  $[\tau_k, \tau_{k+1}]$  is given by

$$\begin{aligned} \int_{\tau_k}^{\tau_{k+1}} |s''_{TC}(t)|^2 dt &= \frac{6}{5h_k} \left( p_k - p_{k+1} + \frac{h_k}{12} (P_k + P_{k+1}) \right)^2 \\ &\quad + \frac{h_k}{24} (3P_k^2 - 2P_k P_{k+1} + 3P_{k+1}^2), \\ &= \mathbf{s}_k^T \mathbf{A}_k \mathbf{s}_k, \end{aligned} \quad (5)$$

where  $\mathbf{s}_k = [z_k, z_{k+1}, p_k, p_{k+1}, P_k, P_{k+1}]^T \in \mathbb{R}^6$ ,

$$\mathbf{A}_k = \frac{1}{30h_k} \begin{bmatrix} 0 & 0 & 0 & 0 & 0 & 0 \\ 0 & 0 & 0 & 0 & 0 & 0 \\ 0 & 0 & 36 & -36 & 3h_k & 3h_k \\ 0 & 0 & -36 & 36 & -3h_k & -3h_k \\ 0 & 0 & 3h_k & -3h_k & 4h_k^2 & -h_k^2 \\ 0 & 0 & 3h_k & -3h_k & -h_k^2 & 4h_k^2 \end{bmatrix}, \quad (6)$$

and  $h_k = \tau_{k+1} - \tau_k$ . By concatenating all intervals as in the form of Eq. (4), a quadratic form is obtained as

$$\int_{\tau_0}^{\tau_n} |s''_{TC}(t)|^2 dt = \sum_{k=0}^{n-1} \int_{\tau_k}^{\tau_{k+1}} |s''_{TC}(t)|^2 dt = \mathbf{s}^T \mathbf{A} \mathbf{s}, \quad (7)$$

where  $\mathbf{A} \in \mathbb{R}^{(3n+3) \times (3n+3)}$  is constructed in the same way as  $\mathbf{A}_k$ . Similarly, the constraint  $s_{TC} \in S_4^2(\boldsymbol{\tau})$  can be rewritten as

$$12(z_k - z_{k+1}) + 6h_k(p_k + p_{k+1}) + h_k^2(P_k - P_{k+1}) = 0, \quad (8)$$

for all  $k \in \{0, 1, \dots, n-1\}$ . By denoting the all constraints [Eq. (8),  $s_{\text{TC}}(\tau_k) = u(\tau_k)$ , and  $s'_{\text{TC}}(\tau_k) = u'(\tau_k)$  for all  $k$ ] as a matrix  $\mathbf{E} \in \mathbb{R}^{(3n+2) \times (3n+3)}$  and  $\mathbf{b} \in \mathbb{R}^{3n+2}$ , Eq. (3) is discretized as

$$\underset{\mathbf{s} \in \mathbb{R}^{3n+3}}{\text{minimize}} \quad \frac{1}{2} \mathbf{s}^T \mathbf{A} \mathbf{s} \quad \text{subject to} \quad \mathbf{E} \mathbf{s} = \mathbf{b}. \quad (9)$$

The solution to this problem is obtained by solving the Karush–Kuhn–Tucker (KKT) system,

$$\mathbf{K} \boldsymbol{\xi} - \tilde{\mathbf{b}} = \mathbf{0}, \quad (10)$$

where

$$\boldsymbol{\xi} = \begin{bmatrix} \mathbf{s} \\ \boldsymbol{\nu} \end{bmatrix}, \quad \mathbf{K} = \begin{bmatrix} \mathbf{A} & \mathbf{E}^T \\ \mathbf{E} & \mathbf{O} \end{bmatrix}, \quad \tilde{\mathbf{b}} = \begin{bmatrix} \mathbf{0} \\ \mathbf{b} \end{bmatrix}, \quad (11)$$

and  $\boldsymbol{\nu} \in \mathbb{R}^{3n+2}$  is a KKT multiplier. From the optimal solution to the discrete problem  $\mathbf{s}^*$ , the corresponding continuous function  $s_{\text{TC}}^* \in S_4^2(\boldsymbol{\tau})$  is recovered as

$$s_{\text{TC}}^*(t) = s_{\text{TC}k}^*(t) = [1, \eta, \eta^2, \eta^3, \eta^4]^T \mathbf{L}_k \mathbf{s}_k^*, \quad (12)$$

for  $t \in [\tau_k, \tau_{k+1}]$  ( $k = 0, 1, \dots, n-1$ ), where

$$\mathbf{L}_k = \frac{1}{12} \begin{bmatrix} 12 & 0 & 0 & 0 & 0 & 0 \\ 0 & 0 & 12h_k & 0 & 0 & 0 \\ 0 & 0 & 0 & 0 & 6h_k^2 & 0 \\ 0 & 0 & -12h_k & 12h_k & -8h_k^2 & -4h_k^2 \\ 0 & 0 & 6h_k & -6h_k & 3h_k^2 & 3h_k^2 \end{bmatrix}, \quad (13)$$

and  $\eta = (t - \tau_k)/h_k \in [0, 1]$ .

### 3.2. Best interpolation points for tangentially constrained spline

Although the tangentially constrained spline  $s_{\text{TC}}$  proposed in the previous subsection can avoid undershoot, its smoothness is sacrificed for most of the choices of tangential points  $\boldsymbol{\tau}$ . In other words, the tangentially constrained spline is smooth only when appropriate tangential points are chosen as the interpolation points. Based on this observation, a method of optimizing tangential points is also proposed so that the proposed spline becomes the smoothest one.

The parameter  $\mathbf{s}^*$  obtained by solving the KKT system in Eq. (10) corresponds to the smoothest tangentially constrained spline  $s_{\text{TC}}^*$  for the given tangential points  $\boldsymbol{\tau}$ . That is, the spline and its parameters can be considered as a function of  $\boldsymbol{\tau}$ . Therefore, an optimization problem of tangential points is formulated as

$$\underset{\boldsymbol{\tau} \in \mathbb{R}^{n+1}}{\text{minimize}} \quad I(\boldsymbol{\tau}) = \frac{1}{2} \mathbf{s}^*(\boldsymbol{\tau})^T \mathbf{A}(\boldsymbol{\tau}) \mathbf{s}^*(\boldsymbol{\tau}), \quad (14)$$

which is a problem of finding tangential points  $\boldsymbol{\tau}$  resulting in the smoothest tangentially constrained spline. Since  $\mathbf{s}^*$  is a solution to Eq. (9) which satisfies the KKT system in Eq. (10), the above problem can be rewritten as a KKT constrained form:

$$\underset{\boldsymbol{\xi} \in \mathbb{R}^{n+1}}{\text{minimize}} \quad \frac{1}{2} \boldsymbol{\xi}^T \tilde{\mathbf{A}}(\boldsymbol{\tau}) \boldsymbol{\xi} \quad \text{subject to} \quad \mathbf{K}(\boldsymbol{\tau}) \boldsymbol{\xi} - \tilde{\mathbf{b}}(\boldsymbol{\tau}) = \mathbf{0}, \quad (15)$$

where  $\tilde{\mathbf{A}} = [[\mathbf{A}, \mathbf{O}]^T, [\mathbf{O}, \mathbf{O}]^T]^T$ . Note that the objective function  $\boldsymbol{\xi}^T \tilde{\mathbf{A}}(\boldsymbol{\tau}) \boldsymbol{\xi} = \mathbf{s}^T \mathbf{A}(\boldsymbol{\tau}) \mathbf{s}$  becomes  $\mathbf{s}^{*T} \mathbf{A}(\boldsymbol{\tau}) \mathbf{s}^*$  when the KKT constraint in Eq. (15) is satisfied.

In order to solve this non-linear optimization problem, a gradient-based optimization method is considered in this paper. Then, the gradient of the cost function  $\nabla_{\boldsymbol{\tau}} I(\boldsymbol{\tau})$  is required. However, its direct computation based on the chain rule involves the

Jacobian matrix  $\partial \boldsymbol{\xi}^* / \partial \boldsymbol{\tau}$  which can be quite costly. Therefore, the adjoint-state method [28, 29] is adopted for computing the gradient without the Jacobian matrix.

Let the cost and constraint of Eq. (15) be compactly written as  $f(\boldsymbol{\xi}, \boldsymbol{\tau}) = (1/2) \boldsymbol{\xi}^T \tilde{\mathbf{A}}(\boldsymbol{\tau}) \boldsymbol{\xi}$  and  $g(\boldsymbol{\xi}, \boldsymbol{\tau}) = \mathbf{K}(\boldsymbol{\tau}) \boldsymbol{\xi} - \tilde{\mathbf{b}}(\boldsymbol{\tau})$ . Then, the Lagrangian associated with Eq. (15) is given by

$$\mathcal{L}(\boldsymbol{\xi}, \boldsymbol{\lambda}, \boldsymbol{\tau}) = f(\boldsymbol{\xi}, \boldsymbol{\tau}) - \boldsymbol{\lambda}^T g(\boldsymbol{\xi}, \boldsymbol{\tau}), \quad (16)$$

where  $\boldsymbol{\lambda} \in \mathbb{R}^{3n+3}$  is an adjoint variable. If  $\boldsymbol{\xi}$  satisfying the KKT system, denoted by  $\boldsymbol{\xi}^*$ , is obtained,  $g(\boldsymbol{\xi}^*, \boldsymbol{\tau}) = \mathbf{0}$ . Therefore,

$$\mathcal{L}(\boldsymbol{\xi}^*, \boldsymbol{\lambda}, \boldsymbol{\tau}) = f(\boldsymbol{\xi}^*, \boldsymbol{\tau}) = I(\boldsymbol{\tau}). \quad (17)$$

Then, the gradient  $\nabla_{\boldsymbol{\tau}} I(\boldsymbol{\tau})$  can be represented as

$$\begin{aligned} \nabla_{\boldsymbol{\tau}} I(\boldsymbol{\tau}) &= \nabla_{\boldsymbol{\tau}} \mathcal{L}(\boldsymbol{\xi}^*, \boldsymbol{\lambda}, \boldsymbol{\tau}) \\ &= \left( \frac{\partial f}{\partial \boldsymbol{\xi}} \frac{\partial \boldsymbol{\xi}^*}{\partial \boldsymbol{\tau}} + \frac{\partial f}{\partial \boldsymbol{\tau}} - \boldsymbol{\lambda}^T \left( \frac{\partial g}{\partial \boldsymbol{\xi}} \frac{\partial \boldsymbol{\xi}^*}{\partial \boldsymbol{\tau}} + \frac{\partial g}{\partial \boldsymbol{\tau}} \right) \right)^T \\ &= \left( \left( \frac{\partial f}{\partial \boldsymbol{\xi}} - \boldsymbol{\lambda}^T \frac{\partial g}{\partial \boldsymbol{\xi}} \right) \frac{\partial \boldsymbol{\xi}^*}{\partial \boldsymbol{\tau}} + \frac{\partial f}{\partial \boldsymbol{\tau}} - \boldsymbol{\lambda}^T \frac{\partial g}{\partial \boldsymbol{\tau}} \right)^T. \end{aligned} \quad (18)$$

As mentioned in the previous paragraph, the computationally expensive part is  $\partial \boldsymbol{\xi}^* / \partial \boldsymbol{\tau}$ , which is eliminated when  $\boldsymbol{\lambda}^*$  is chosen such that

$$\left( \frac{\partial f}{\partial \boldsymbol{\xi}} - \boldsymbol{\lambda}^{*T} \frac{\partial g}{\partial \boldsymbol{\xi}} \right)^T = \mathbf{0}, \quad (19)$$

where this choice of  $\boldsymbol{\lambda}$  does not affect the objective function and its gradient since  $I(\boldsymbol{\tau}) = \mathcal{L}(\boldsymbol{\xi}^*, \boldsymbol{\lambda}, \boldsymbol{\tau}) = \mathcal{L}(\boldsymbol{\xi}^*, \boldsymbol{\lambda}^*, \boldsymbol{\tau})$  as shown in Eq. (17). After some manipulations, this equation reduces to

$$\mathbf{K} \boldsymbol{\lambda}^* = \tilde{\mathbf{A}} \boldsymbol{\xi}^*. \quad (20)$$

Therefore, by using  $\boldsymbol{\xi}^*$  and  $\boldsymbol{\lambda}^*$  which are obtained from Eqs. (10) and (20), respectively, the gradient can be efficiently calculated as

$$\begin{aligned} \nabla_{\boldsymbol{\tau}} I(\boldsymbol{\tau}) &= \nabla_{\boldsymbol{\tau}} \mathcal{L}(\boldsymbol{\xi}^*, \boldsymbol{\lambda}^*, \boldsymbol{\tau}) \\ &= \left( \frac{\partial f}{\partial \boldsymbol{\tau}} - \boldsymbol{\lambda}^{*T} \frac{\partial g}{\partial \boldsymbol{\tau}} \right)^T \\ &= \frac{1}{2} \mathbf{D}_{\mathbf{A}}^T \boldsymbol{\xi}^* - \left( \mathbf{D}_{\mathbf{K}} - \frac{\partial \tilde{\mathbf{b}}}{\partial \boldsymbol{\tau}} \right)^T \boldsymbol{\lambda}^*, \end{aligned} \quad (21)$$

where  $\mathbf{D}_{\mathbf{A}}$  and  $\mathbf{D}_{\mathbf{K}}$  are derivatives corresponding to  $\mathbf{A}$  and  $\mathbf{K}$  as

$$\mathbf{D}_{\mathbf{A}} = \left[ \frac{\partial \tilde{\mathbf{A}}}{\partial \tau_0} \boldsymbol{\xi}, \dots, \frac{\partial \tilde{\mathbf{A}}}{\partial \tau_n} \boldsymbol{\xi} \right], \quad \mathbf{D}_{\mathbf{K}} = \left[ \frac{\partial \mathbf{K}}{\partial \tau_0} \boldsymbol{\xi}, \dots, \frac{\partial \mathbf{K}}{\partial \tau_n} \boldsymbol{\xi} \right]. \quad (22)$$

For the optimization method, the Broyden–Fletcher–Goldfarb–Shanno (BFGS) algorithm is used in this paper [30–33]. The BFGS algorithm is a quasi-Newton method which approximates the inverse Hessian matrix by the following update rule:

$$\mathbf{H}_{i+1} = \mathbf{H}_i + \left( 1 + \frac{\boldsymbol{\gamma}_i^T \mathbf{H}_i \boldsymbol{\gamma}_i}{\boldsymbol{\delta}_i^T \boldsymbol{\gamma}_i} \right) \frac{\boldsymbol{\delta}_i \boldsymbol{\delta}_i^T}{\boldsymbol{\delta}_i^T \boldsymbol{\gamma}_i} - \frac{\mathbf{H}_i \boldsymbol{\gamma}_i \boldsymbol{\delta}_i^T + \boldsymbol{\delta}_i \boldsymbol{\gamma}_i^T \mathbf{H}_i}{\boldsymbol{\delta}_i^T \boldsymbol{\gamma}_i}, \quad (23)$$

where  $\boldsymbol{\delta}_i = \boldsymbol{\tau}_{i+1} - \boldsymbol{\tau}_i$ , and  $\boldsymbol{\gamma}_i = \nabla_{\boldsymbol{\tau}} I(\boldsymbol{\tau}_{i+1}) - \nabla_{\boldsymbol{\tau}} I(\boldsymbol{\tau}_i)$ .

## 4. NUMERICAL EXPERIMENT

In this section, two experiments were performed to confirm the effectiveness of the proposed method. The proposed method was compared with the convention method using the cubic  $C^2$ -spline interpolation. For the end points which are always the central issue in EMD [34], mirrored signals were padded at each end of the signal [35].

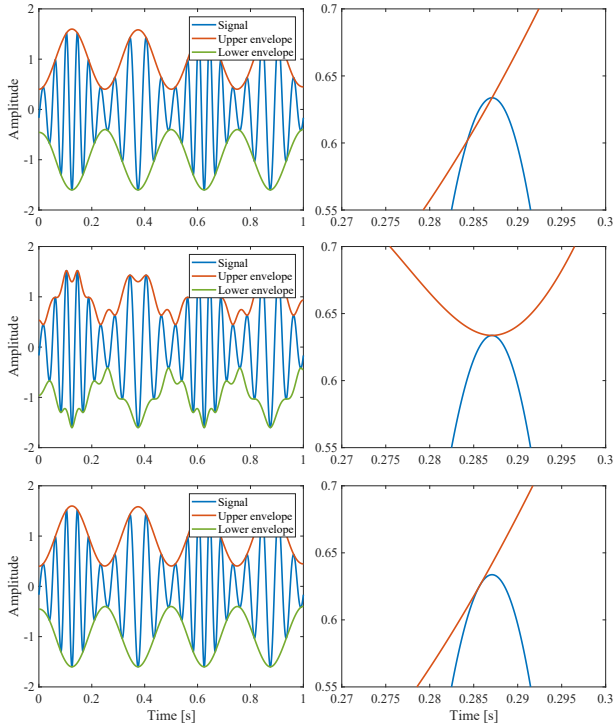


**Fig. 2.** Estimated envelopes based on the spline interpolation methods. Each row shows (from top to bottom) results for the conventional cubic  $C^2$ -spline interpolation, results for the proposed tangentially constrained spline without tangential points optimization, and results for the proposed method. The right column shows the enlargement of each figure in the left column.

#### 4.1. Comparison of envelopes

At first, an envelope estimation problem of a simulated signal,

$$u(t) = (1 - 0.6 \cos(8\pi t)) \cos(40\pi t - 2 \cos(4\pi t)), \quad (24)$$

$t \in [0, 1]$  was considered. The envelopes obtained by the conventional cubic  $C^2$ -spline interpolation and the proposed method are shown in Fig. 2. Although the envelopes obtained by the cubic  $C^2$ -spline interpolation are smooth (top row), they contain undershoots

as seen in the enlarged figure. Such a few amount of undershoots greatly affects the results of EMD in the wrong direction. The envelopes obtained by the proposed method were tangent at interpolation points as expected (middle row), which confirmed the correctness of the proposed formulation in Sec. 3.1. However, the proposed spline itself is not so smooth owing to the tangential constraint. The spline smoothest among the tangentially constrained splines was obtained by the proposed tangential points optimization in Sec. 3.2 as shown in the bottom row. This result indicates that the proposed method can estimate a smooth tangential envelope without the undershoot problem.

#### 4.2. Application to EMD

The proposed method was compared with the conventional method in terms of the results of EMD. EMD was applied to a signal consisting of three components shown in Fig. 3 (a). Results of EMD are shown in Fig. 3 (b) and (c), where the result obtained by the proposed method is in Fig. 3 (b), and that of the conventional method is in Fig. 3 (c). EMD based on the conventional method resulted in four components as shown in Fig. 3(c), which should be the effect of undershoot of the estimated envelopes. On the other hand, EMD with the proposed method correctly recovered the original components because undershoot is avoided in the proposal.

These results in Figs. 2 and 3 suggest that the envelopes estimated by the proposed method have better characteristics than the conventional ones. However, similarly to any other envelope estimation methods [2–21], the proposed method also depends on the condition around the boundary of the signal. That is, the effect from outside of the observed period can reduce the accuracy of the estimation result. Since the proposed method is based on the optimization, an optimal boundary condition might be obtained as an extension of the proposed method. This possibility should be considered in the future works.

### 5. CONCLUSION

In this paper, a tangentially constrained spline for estimating envelopes without the undershoot problem is proposed. It is a quartic  $C^2$ -spline constrained by first derivatives at the tangential points that always satisfy the tangential condition of envelope. A tangential points optimization method is also proposed so that an optimally smooth envelope among the proposed splines is obtained. Future works include considerations of appropriate boundary conditions as discussed in the experimental section.

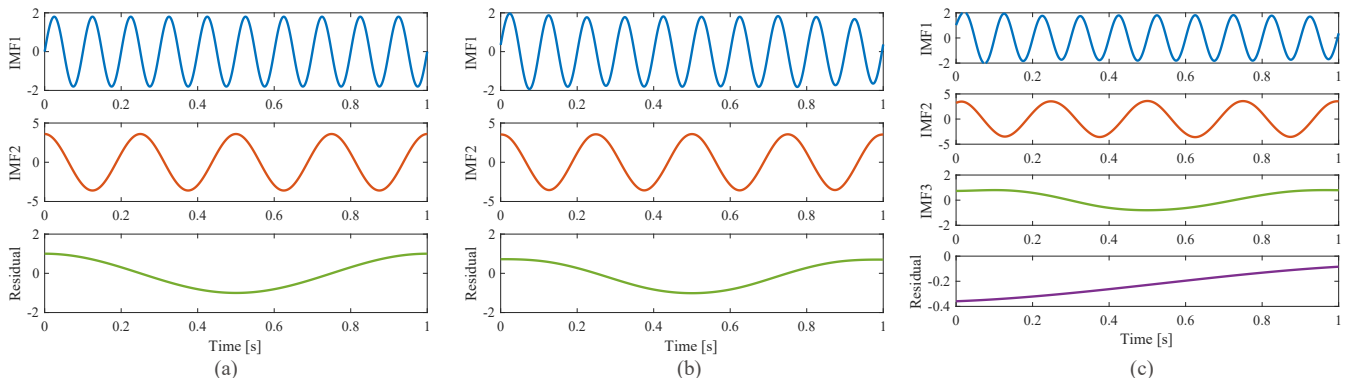


**Fig. 3.** Results of EMD with different envelope estimation methods. Components of the original signal in (a) were decomposed by EMD after mixing. (b) and (c) show the results of EMD based on the proposed method and the conventional method, respectively.

## 6. REFERENCES

- [1] Y. Yang, "A signal theoretic approach for envelope analysis of real-valued signals," *IEEE Access*, vol. 5, pp. 5623–5630, 2017.
- [2] N. E. Huang, Z. Shen, S. R. Long, M. C. Wu, H. H. Shih, Q. Zheng, N.-C. Yen, C. C. Tung, and H. H. Liu, "The empirical mode decomposition and the Hilbert spectrum for nonlinear and non-stationary time series analysis," *Proc. R. Soc. Lond. A*, vol. 454, no. 1971, pp. 903–995, 1998.
- [3] P. Flandrin, G. Rilling, and P. Goncalves, "Empirical mode decomposition as a filter bank," *IEEE Signal. Proc. Let.*, vol. 11, no. 2, pp. 112–114, Feb. 2004.
- [4] G. Rilling and P. Flandrin, "One or two frequencies? The empirical mode decomposition answers," *IEEE Trans. Signal Process.*, vol. 56, no. 1, pp. 85–95, Jan. 2008.
- [5] G. Rilling and P. Flandrin, "Sampling effects on the empirical mode decomposition," *Adv. Adapt. Data Anal.*, vol. 01, no. 01, pp. 43–59, 2009.
- [6] Q. Wu and S. D. Riemenschneider, "Boundary extension and stop criteria for empirical mode decomposition," *Adv. Adapt. Data Anal.*, vol. 02, no. 02, pp. 157–169, 2010.
- [7] N. E. Huang, M.-L. Wu, W. Qu, S. R. Long, and S. S. P. Shen, "Applications of Hilbert–Huang transform to non-stationary financial time series analysis," *Appl. Stochastic Models Bus. Ind.*, vol. 19, no. 3, pp. 245–268, 2003.
- [8] A. O. Boudraa and J. C. Cexus, "EMD-based signal filtering," *IEEE Trans. Instrum. Meas.*, vol. 56, no. 6, pp. 2196–2202, Dec. 2007.
- [9] N. E. Huang and Z. Wu, "A review on Hilbert–Huang transform: Method and its applications to geophysical studies," *Rev. Geophys.*, vol. 46, no. 2, 2008.
- [10] V. Bajaj and R. B. Pachori, "Classification of seizure and nonseizure EEG signals using empirical mode decomposition," *IEEE Trans. Inf. Technol. Biomed.*, vol. 16, no. 6, pp. 1135–1142, Nov. 2012.
- [11] Y. Lei, J. Lin, Z. He, and M. J. Zuo, "A review on empirical mode decomposition in fault diagnosis of rotating machinery," *Mech. Syst. Sig. Process.*, vol. 35, no. 1, pp. 108–126, 2013.
- [12] T. Tanaka and D. P. Mandic, "Complex empirical mode decomposition," *IEEE Signal. Proc. Let.*, vol. 14, no. 2, pp. 101–104, Feb. 2007.
- [13] G. Rilling, P. Flandrin, P. Goncalves, and J. M. Lilly, "Bivariate empirical mode decomposition," *IEEE Signal. Proc. Let.*, vol. 14, no. 12, pp. 936–939, Dec. 2007.
- [14] N. Rehman and D. P. Mandic, "Multivariate empirical mode decomposition," *Proc. R. Soc. Lond. A*, vol. 466, no. 2117, pp. 1291–1302, 2010.
- [15] Z. Wu and N. E. Huang, "Ensemble empirical mode decomposition: A noise-assisted data analysis method," *Adv. Adapt. Data Anal.*, vol. 01, no. 01, pp. 1–41, 2009.
- [16] Q. Chen, N. E. Huang, S. D. Riemenschneider, and Y. Xu, "A B-spline approach for empirical mode decompositions," *Adv. Comput. Math.*, vol. 24, no. 1, pp. 171–195, 2006.
- [17] Z. Xu, B. Huang, and K. Li, "An alternative envelope approach for empirical mode decomposition," *Digital Signal Process.*, vol. 20, no. 1, pp. 77–84, 2010.
- [18] S. R. Qin and Y. M. Zhong, "A new envelope algorithm of Hilbert–Huang transform," *Mech. Syst. Sig. Process.*, vol. 20, no. 8, pp. 1941–1952, 2006.
- [19] L. Yang, Z. Yang, L. Yang, and P. Zhang, "An improved envelope algorithm for eliminating undershoots," *Digital Signal Process.*, vol. 23, no. 1, pp. 401–411, 2013.
- [20] X. Hu, S. Peng, and W. L. Hwang, "EMD revisited: A new understanding of the envelope and resolving the mode-mixing problem in AM-FM signals," *IEEE Trans. Signal Process.*, vol. 60, no. 3, pp. 1075–1086, Mar. 2012.
- [21] W. Zhu, H. Zhao, D. Xiang, and X. Chen, "A flattest constrained envelope approach for empirical mode decomposition," *PLoS One*, vol. 8, no. 4, pp. 1–12, 2013.
- [22] Y. Washizawa, T. Tanaka, D. P. Mandic, and A. Cichocki, "A flexible method for envelope estimation in empirical mode decomposition," in *Proc. 10th Int. Conf. Knowl.-Based Intell. Inf. Eng. Syst. (KES 2006)*, Bournemouth, UK, 2006, pp. 1248–1255.
- [23] B. Huang and A. Kunoth, "An optimization based empirical mode decomposition scheme," *J. Comput. Appl. Math.*, vol. 240, pp. 174–183, 2013.
- [24] L. Yang, Z. Yang, F. Zhou, and L. Yang, "A novel envelope model based on convex constrained optimization," *Digital Signal Process.*, vol. 29, pp. 138–146, 2014.
- [25] G. Wahba, *Spline Models for Observational Data*, Society for Industrial and Applied Mathematics, Philadelphia, PA, 1990.
- [26] R. T. Rato, M. D. Ortigueira, and A. G. Batista, "On the HHT, its problems, and some solutions," *Mech. Syst. Sig. Process.*, vol. 22, no. 6, pp. 1374–1394, 2008.
- [27] W. Heß and J. W. Schmidt, "Positive quartic, monotone quintic  $C^2$ -spline interpolation in one and two dimensions," *J. Comput. Appl. Math.*, vol. 55, no. 1, pp. 51–67, 1994.
- [28] G. Chavent, "Identification of functional parameters in partial differential equations," in *Proc. Jt. Autom. Control Conf.*, Austin, Texas, 1974, pp. 31–48.
- [29] R.-E. Plessix, "A review of the adjoint-state method for computing the gradient of a functional with geophysical applications," *Geophys. J. Int.*, vol. 167, no. 2, pp. 495–503, 2006.
- [30] C. G. Broyden, "The convergence of a class of double-rank minimization algorithms 1. General considerations," *IMA J. Appl. Math.*, vol. 6, no. 1, pp. 76–90, 1970.
- [31] R. Fletcher, "A new approach to variable metric algorithms," *Comput. J.*, vol. 13, no. 3, pp. 317–322, 1970.
- [32] D. Goldfarb, "A family of variable-metric methods derived by variational means," *Math. Comput.*, vol. 24, no. 109, pp. 23–26, 1970.
- [33] D. F. Shanno, "Conditioning of quasi-Newton methods for function minimization," *Math. Comput.*, vol. 24, no. 111, pp. 647–656, 1970.
- [34] N. E. Huang, *Hilbert–Huang transform and its applications*, World Scientific, Singapore, 2005.
- [35] G. Rilling, P. Flandrin, and P. Goncalves, "On empirical mode decomposition and its algorithms," in *Proc. IEEE-EURASIP Workshop Nonlinear Signal Image Process.*, Grado, Italy, 2003.